Self-Adaptive Blind Super-Resolution Image Reconstruction

Yunfei Bai, Jing Hu, Yupin Luo
Tsinghua National Laboratory for Information Science and Technology (TNList)
Department of Automation Tsinghua University
Beijing, China 10084

***Abstract*—Super-resolution (SR) image reconstruction is a rapidly developing area in image processing. Especially, blind SR can generate high space resolution image without requiring priori information of the point spread function (PSF). In this paper, we propose a self-adaptive blind super-resolution image reconstruction approach which is based on multiple images. Our method can adaptively choose the parameter of regularization term. The quality of resulting image especially in the respect of edge-preserving property is better than approaches such as maximum a posteriori estimation (MAP) tested with practical examples. We employ Lorentzian function as spread coefficient and partial differential function as regularization term of resulting image. A generalized version of the eigenvector-based alternating minimization (EVAM) constraint is used to regularize PSF and estimate resulting image and PSF simultaneously. In addition, in order to achieve self-adaptive regularization terms parameter choosing, we also present a new robust no-reference image quality assessment method which provides blurring and ringing effect assessment value as feedback.**

Keywords-super-resolution image reconstruction; blind SR; no-reference image quality assessment

I. INTRODUCTION

The quality of images can be significantly affected by the situation when capturing. The goal of super-resolution (SR) image reconstruction is to promote the space resolution of captured original images through software.

After the first effective approach proposed by Tsai et al. [1] to solve this ill-posed problem, there are diverse methods to handle SR problem which can be classified into two groups: the multiple frames based approaches and single frame based approaches [2] [3]. For multiple frames based approaches, spatial domain and frequency domain [4] are two major directions and the former one is more popular these years as it can be applied to more general images with motion blur and noise to produce higher quality result. Some popular approaches belonging to spatial ones are projection-onto-convex-sets (POCS) [5], iterative back-projection (IBP) [6] [7], maximum a posteriori estimation (MAP) [8] [9]. However, the deficiencies of these methods are in that they all need priori information of the point spread function (PSF) which is always difficult to get in practical situation. Therefore, to solve this problem, the blind SR method [10] is proposed which combines the image registration, image restoration and PSF estimation into one framework. The method uses partial differential equation (PDE) as the regularization term of the high resolution image to preserve the edges while suppressing noise. However, the parameter of the regularization term which is significant in determining the smoothness of the image should be adjusted manually, which increases the indefinability in generating high quality images with detailed texture.

The method we propose here is a self-adaptive blind super-resolution image reconstruction approach based on multiple frames. In the paper, PDE framework and eigenvector-based alternating minimization (EVAM) constraint are used as the regularization term. In addition, we also design a novel image quality assessment method without reference image for adaptively choosing parameter of this blind super-resolution algorithm.

II. OVERVIEW

A. Mathematical Model

SR can be seen as the opposite procedure of observation model in imaging system. The low resolution images are captured through the process of blurring, distortion, down-sampling as well as system noise. The blurring-warping model is an appropriate mathematical model in SR [11] and can be represented as

$$L_k = D[M_k(B_k * H)] + N_k, \tag{1}$$

where L_k is the captured frame k^{th} low resolution image with the size of $m \times n$. H is the corresponding high resolution image, and it will have the size of $qm \times qn$ when the resolution enhancement factor is q. B_k is the PSF of the k^{th} frame which convolves with the high resolution image and determines the type of blur. In addition, M_k is the motion and distortion operator, D is the down-sampling operator, and N_k denotes the system noise.

In this paper, we only consider the motion of global translation, and assume that the PSF of the imaging system is constant. Therefore, an extended PSF can be defined as E_k, which incorporates convolution with blur operator as well as motion and distortion into one operation. And E_k is a center translational blur function convoluted with the high resolution image. Accordingly, (1) can be rewritten as

$$L_k = D(E_k * H) + N_k, \tag{2}$$

With this mathematical model, the SR image reconstruction problem is to solve H, while estimating the extended PSF E_k and system noise N_k, given low resolution images $L_k$and down-sampling operator D.

978-1-4244-6516-3/10/$26.00 ©2010 IEEE

B. Approach Pipeline

Our approach consists of two main stages. First, PDE is used as the regularization term of high resolution image, which contains Lorentzian function as spread coefficient. In another aspect, we use EVAM constraint as the regularization term of the extended PSF. Alternating minimization algorithm is used to minimize the cost function. Second, we propose a no-reference image quality assessment method which considers the effects of blurring and ringing to guide the choice of parameters in the regularization term. In this way it is possible to preserve the details of the image since the parameter significantly determines the smoothness of the resulting image.

III. ALGORITHM

A. Cost Function

In order to achieve a stable solution of formula (2), we utilize a regularization approach to solve this problem. Some specific type of regularization terms to constrain H as well as E_k are employed separately. Besides, we use Lagrange multiplier framework to resolve this problem by minimizing the energy function shown in (3).

$$E(H, E_1, E_2, ..., E_n) = \frac{1}{2}\sum_{k=1}^{n} \|D(E_k * H - L_k)\|^2 + \lambda Q(H) + \gamma R(E_1, E_2, ..., E_n), \tag{3}$$

And the constraints are

$$0 \le a \le H(x, y) \le b < \infty, (x, y) \in \Omega, \tag{4}$$

$$0 \le E_k, and \sum_{(u,w)\in\Delta} E_k(u, w) = 1. \tag{5}$$

While minimizing the energy function $E(H, E_1, E_2, ..., E_n)$, we estimate H and E_k in n frames respectively. $Q(H)$ is the regularization term of the high resolution image while $R(E_1, E_2, ..., E_n)$ is the regularization term of extended PSF. λ and γ are parameters which control the degree of smoothness of each term. In the constraint, $H(x, y)$ stands for the intensity of the pixel at coordinate (x, y) and it is limited in the range of a to b. Ω is the space domain of the high resolution image. And Δ stands for the space domain of extended PSF.

The first term on the right side of equation (3) reflects the approximation of high resolution image estimation. $Q(H)$ determines the image quality of preserving detailed texture. And it's the contribution of our work is to choose appropriate type of $Q(H)$ as well as find an approach to adaptively choose the parameter.

B. Image Regularization

As to image regularization term $Q(H)$, Pan et al. [12] employs the Markov Random Field and Gibbs Model as the regularization term. In addition, PDE is used in image processing area these years as it can preserve the edge of the image while suppressing noise. Anisotropic spread PDE which is widely used in heat conduction is proposed by Perona et al. [13] to solve image processing problem and the equation used is (6).

$$\frac{\partial H(x, y, t)}{\partial t} = div(c(|\nabla H|)\nabla H). \tag{6}$$

In this equation, t is an introduced parameter representing time, and the first image is represented by $t = 0$. ∇H is the grads of the image and c is a spread coefficient which is an edge-stopping function. The value of c tends to zero when it comes to the edge of the image to preserve the details. But when it comes to non-edge area, the value of c is larger to suppress the noise.

According to the variation method, solving (6) is equal to minimizing the energy function (7), thus the regularization term can be written as in (8) and the relationship between ρ and c is described in (9).

$$\min_H E(H) = \int_\Omega \rho(|\nabla H|)d\Omega, \tag{7}$$

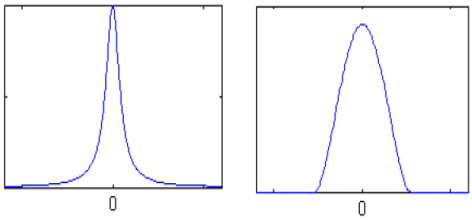

(a) (b)

Fig. 1. Spread function image

$$Q(H) = \int_\Omega \rho(|\nabla H|)d\Omega, \tag{8}$$

$$c(x) = \rho'(x)/x. \tag{9}$$

We employ the function type Lorentzian as in (10) and (11) and set K to be 3. As we can see the functional image of Lorentzian in Fig. 1(a), the peak of this function is pointed which concentrates around zero and thus can preserve the details as far as possible compared with Tukey function depicted in Fig. 1(b).

$$c(x, K) = \frac{2}{2K + x^2}, \tag{10}$$

$$\rho(x, K) = \log(1 + \frac{x^2}{2K}). \tag{11}$$

C. Extended PSF Regularization

In order to preserve the consistency among PSF of different channels while preventing overfitting between PSF estimation and noise in observed images, a generalized regularization term is utilized to constrain the extended PSF E_k. Gürelli et al. [14] devise the EVAM constraint to calculate extended PSF. And this method is utilized in blind restoration of multiple frames [15]. According to the EVAM constraint we have constraint like (12) among which Y_k stands for image with

blur and distortion but without down-sampling. So Y_k and the observed image L_k satisfies $L_k = D(Y_k)$.

$$Y_i * E_j - Y_j * E_i = 0, 1 \le i < j \le n. \tag{12}$$

Based on (12), we can deduct the equation (13) according to multiresolution approximation theory in [16] and get a generalized regularization term as in (14) on considering specific noise model.

$$D_l(Y_i) * D_l(E_j) - D_l(Y_j) * D_l(E_i) = 0, 1 \le i < j \le p, \tag{13}$$

$$R(E_1, ..., E_n) = \frac{1}{2} \sum_{1 \le i < j \le n} \|L_i * D(E_j) - L_i * D(E_i)\|^2. \tag{14}$$

D. Alternating Minimization Algorithm

According to the regularization terms expressed in the above sections, we can get an integrated form of cost function as in (15) to minimize.

$$\begin{aligned} E(H, E_1, ..., E_n) &= \tfrac{1}{2} \sum_{k=1}^{n} \|D(E_k * H) - L_k\|^2 \\ &+ \lambda \int_{\Omega} \rho(|\nabla H|) d\Omega + \tfrac{1}{2} \gamma \sum_{1 \le i < j \le n} \|L_i * D(E_j) - L_i * D(E_i)\|^2 \end{aligned} \tag{15}$$

This energy function is not a convex function. Šroubek et al. [17] point that when E_k is fixed, $E(H, E_1, ..., E_n)$ is a convex function for H. While in another aspect, when H is fixed, $E(H, E_1, ..., E_n)$ is quadrics. Therefore, we employ the alternating minimization algorithm to solve this optimization problem. For the initial value H^0 which is the bilinear interpolation result of one low resolution image, the alternating minimization algorithm alternates between the following two steps

$$E_k^n = \arg\min_{E_k} E(H^{n-1}, E_k), \tag{16}$$

$$H^n = \arg\min_{H} E(H, E_k^n). \tag{17}$$

E. No-reference Image Assessment

Image quality assessment has always been a bottleneck in image processing, of which the methods can be classified into two categories, subjective approaches and objective approaches. What is more, the objective image quality assessment methods can again be classified as full-reference methods, reduced-reference methods and no-reference methods [18]. Some popular full-reference approaches are mean square error (MSE), peak signal to noise ratio (PSNR), intense signal to noise ratio (ISNR), etc. No-reference methods use no-reference images and only employ pixels information of the observed image to generate a criterion thus suits in more situations. And [19] is a survey about no-reference image quality assessment methods. However, no-reference methods are not in accord with actual human vision sometimes.

As to SR area, blurring and ringing effects are two main factors that affect quality of resulting images seriously. As blurring effect is characterized by an increase of the spread of edges and spatial details, we can define degree of blur of image as

$$blurmeasure = \frac{\sum_{i=1}^{m} \sum_{j=1}^{n} d_{ij}}{\sum_{i=1}^{m} l_i}. \tag{18}$$

The height and width of the image are m and n respectively, and $d_{i,j}$ stands for the width of j^{th} edge at row i, l_i stands for the number of edges at row i. The Canny operator is used to locate the edges of image and the spread of edge at each row is defined as in [20].

On the other hand, ringing effect is caused by the quantization or truncation of the high frequency coefficients known as the Gibbs phenomenon. Compared with the full-reference ringing metric in [20], we propose a no-reference approach that gives the ringing effect assessment result through calculating intensity of local haloes near sharp objects' edges. And the calculation is described as in (19). We first use Canny operator to find edges of contents and then fix the possible ringing area by dilatation of edges in horizontal and vertical direction. We define this possible ringing area as $RingMask$ which is a matrix of the same size with the original image. Next, Sobel operator with small threshold is utilized to generate a binary image of extended edges denoted as PE which consists of real contents' edges and rings near sharp edges. Then, Sobel operator with larger threshold is used to generate a binary image consisting of contents' edges only which is denoted as AE. The differences between these two binary images are possible rings of image. The and operation denoted as $\&$ is carried out between the $RingMask$ and $(PE - AE)$ to get actual ringing area. To calculate the intensity of ringing effect, the ratio of the number of pixels of rings to pixels of whole image TN is employed as the ringing effect assessment value,and $Num[]$ stands for the number of element with value of 1 in the matrix.

$$ringmeasure = \frac{Num[RingMask \& (PE - AE)]}{TN}. \tag{19}$$

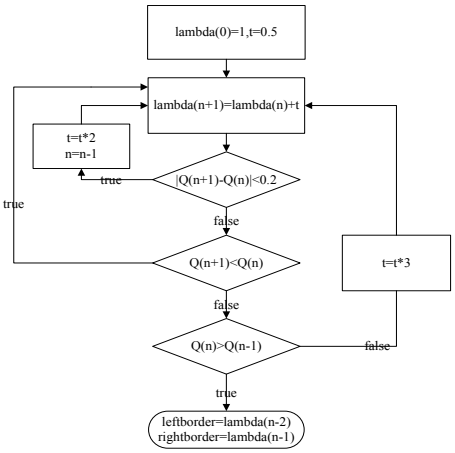

Figure 2. Finding optimal regularization term paramter interval algorithm

Linearly combining the blurring and ringing measure approaches, we obtain the image assessment Q as

$$Q = blurmeasure + 15 * ringmeasure \tag{20}$$

where $blurmeasure$ and $ringmeasure$ stands for blurring measure and ringing measure respectively. And the image quality is better when the assessment value is smaller.

F. Self-adaptive Parameter Choosing

As the value of quality assessment is a function of image regularization term parameter λ, we can employ the idea of function optimization to search the optimal parameter. The ringing effect and blurring effect are serious when λ is too small and large respectively, thus the quality assessment value is approximately a convex function. If we can find an approximate convex interval containing optimal solution of λ, then it is possible to utilize nonlinear programming to search the optimal λ. The steps of finding the interval containing optimal solution are as follows and the pipeline is described in Fig. 2.

a) Initial λ is set as 1. The variation step of λ is denoted as t and is set to be 0.5 initially. We first generate the resulting image using this parameter and get quality assessment result Q.

b) The next λ is the current λ plus step t, that is $\lambda_{n+1} = \lambda_n + t$. And the current quality assessment result is Q_{n+1}.

c) If the difference between Q_n and Q_{n+1} is less than the threshold, then the step multiplies by two, that is $t = t \times 2$, then go back to step b) with the suffix count of Q and λ minus one. Else, go to step d) or e).

d) If Q_{n+1} is larger than Q_n, at the same time, Q_n is larger than Q_{n-1}, then the left border is λ_{n-2} and right border is λ_{n-1}. On the other hand, if Q_{n+1} is larger than Q_n, and Q_n is smaller than Q_{n-1}, then the step multiplies by three, that is $t = t \times 3$, and go to step b).

e) If Q_{n+1} is smaller than Q_n, then go back to step b).

IV. EXPERIMENTS AND PERFORMANCE

We first demonstrate validation of image quality assessment approach on blurring and ringing effect separately. Next, we use two sets of experiments to show that our algorithm can find optimal parameter of regularization terms and generate high quality image. The first one is based on simulated data generated from high resolution image with global translation and blur. The second set of experiments involves a sequence of low resolution images obtained from real video sequence.

In all these experiments, the resolution enhancement factor is set to 4. The iteration of alternating minimization algorithm is set to 1. And the parameter of regularization term of extended PSF γ is set to 0.001.

A. Image Quality Assessment

The proposed no-reference image quality assessment is applied to simulated images which are with different degrees of blur generated through middle filter. The change of quality value on blurring along with middle filter size is depicted in Fig. 3.

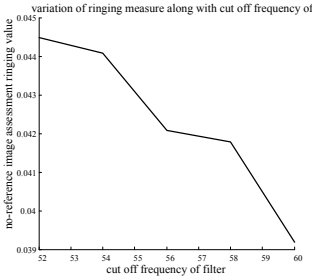

Figure 3. Blurring value changes with size of filter

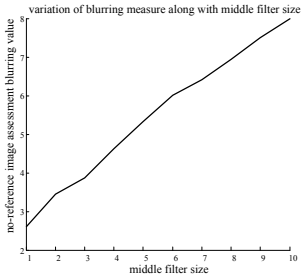

Figure 4. Ringing value changes with cut off frequency of filter

We utilize images generated by low pass filter as test data to demonstrate the effectiveness of ringing effect assessment. When cutoff frequency gets smaller, the ringing effect will become more serious. The relationship between ringing effect assessment value and cutoff frequency of ideal low pass filter is shown in Fig. 4.

B. Finding Optimal Regularization Term Parameter

In the experiment with simulated images, we use original high resolution calender image of size 204×256 in Fig. 6(a) to generate 25 low resolution images of size 51×64 as in Fig. 5(e) by using PSF of size 12×12 in Fig. 5(f) and shifting as [0,0; 0,1; 0,2; 0,3; 0,4; 1,0; 1,1; 1,2; 1,3; 1,4; 2,0; 2,1; 2,2; 2,3; 2,4; 3,0; 3,1; 3,2; 3,3; 3,4; 4,0; 4,1; 4,2; 4,3; 4,4] with additive Gaussian noise. The quality value curve of resulting images generated by our algorithm with different regularization term parameter λ is shown in Fig. 5(g). The value of first λ is set as 0.75, and added by 0.25 each time.

After 10 iterations, the left and right border of interval our algorithm choose is 1.5 and 9 seperately. Then nonlinear programming algorithm sets λ to be 3.2705 and the resulting image is shown in Fig. 5(c). We also generate an image using MAP method which is shown in Fig. 5(d). The first frame of simulated low resolution image is bilinear interpolated and depicted in Fig. 5(b).

To illustrate better perfomance of our approach, we give the measurement calculated by our no-reference image quality assessment as well as PSNR on resulting images generated by our approach and MAP, and the comparison is shown in Table 1.

TABLE I
COMPARISON OF OUR APPROACH AND MAP

Performance comparison	Assessment value	
	PSNR	Our no-reference image quality assessment
Our approach	29.9548dB	3.0463
MAP	26.6860dB	5.0318

C. Demonstration With Real Data

We also use real data to illustrate effectiveness of our approach. We apply our approach to real 16 color low resolution

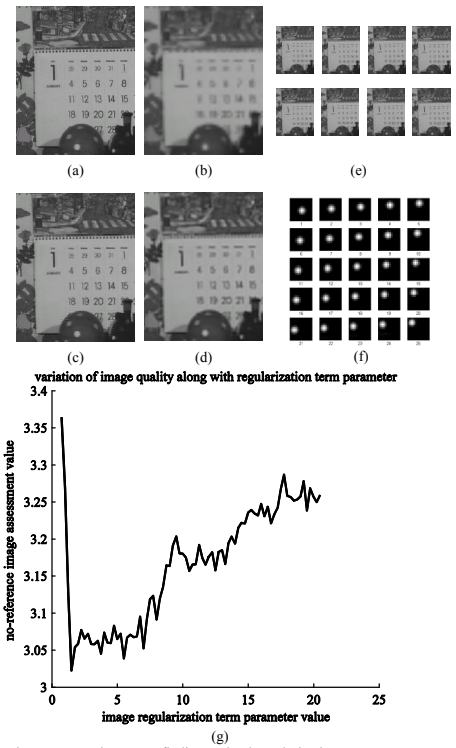

Figure 5. Experiments on finding optimal regularization term parameter

images of size 51×64 derived from a video sample which are depicted in Fig. 6(c). The generated image through our approach is shown in Fig. 6(a). Iteration of our approach is 7 and the left and right border of interval is 2.5 and 4 respectively. And Fig. 6(b) shows the bilinear interpolation result of first frame low resolution image.

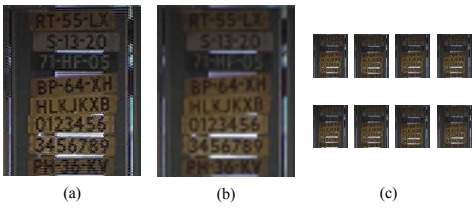

Figure 6. Experiments with real data

V. CONCLUSION AND DISCUSSION

In this article, we propose a self-adaptive multiple frames based blind SR approach which can adaptively choose parameter of regularization terms while generating high space resolution image with edge-preserving property. To achieve self-adaptive parameter chosen, we also propose a robust no-reference image quality assessment which focuses on blurring and ringing effect to provide feedback to regularization terms.

Our approach can effectively generate high resolution image from a set of images with global translation, however, there is still a need of further research to deal with scene containing moving objects. In addition, like other popular methods, our approach requires iterated calculation which is computational intensive. Therefore, modifying the algorithm to promote the efficiency to achieve real-time super-resolution image reconstruction is a promising research direction.

REFERENCES

[1] R. Y. Tsai and T. S. Huang, *Multiple frame image reconstruction and registration*. Advances in Computer Vision and Image Processing. JAI Press Inc., Greenwich, CT, pp. 317-339,1999.

[2] J. D. Ouwerkerk, *Image super-resolution survey* Image and Vision Computing, 24(1), pp.1039-1052, 2006.

[3] D. Glasner, S. Bagona and M. Irani, *Super-resolution from a single image*, International Conference on Computer Vision (ICCV), October 2009.

[4] S. P. Kim and W. Y. Su, *Recursive high-resolution reconstruction of blurred multiframe images*, IEEE Transactions on Image Processing, 2(4), pp. 534-539, 1993.

[5] K. Sauer and J. Allebach, *Iterative reconstruction of band-limited images from non-uniformly spaced samples*, IEEE Transactions on Circuits and Systems, CAS-34(12), pp.1497-1505, 1987.

[6] M. Irani and S. peleg, *Motion analysis for image enhancement: resolution, occlusion, and transparency*, Journal of Visual Communication and Image Representation, 4, pp.324-335, 1997.

[7] M. B. Sauer, Z. Lin and B. Wilburn *Super-resolution in the detector layout domain*, Internation Conference on Computer Vision (ICCV) 2007.

[8] R. R. Schultz and R. L. Stevenson, *A Bayesian approach to image expansion for improved definition*, IEEE Transactions on Image Processing, 3(3), pp.233-242, 1994.

[9] R. C. Hardie, k. J. Barnard and E. E. Armstrong, *Joint MAP registration and high-resolution image estimation using a sequence of undersampled images*, IEEE Transactions on Image Processing, 6, pp.1621-1633, 1997.

[10] F. Šroubek and J. Flusser and E. E. Armstrong, *Multichannel blind iterative image restoration*, IEEE Transactions on Image Processing, 12(9), pp.1094-1106, 2003.

[11] Z. Wang and F. Qi, *On ambiguities in super-resolution modeling*, IEEE Signal Processing Letters, Vol.11, No.8, Aug. 2004.

[12] R. Pan and S.J. Reeves, *Efficient Huber-markov edge-preserving image restoration*, IEEE Transactions on Image Processing, pp. 3728-3725, 2006.

[13] P. Perona and J. Malik, *Scale-space and edge detection using anisotropic diffusion*, IEEE Transactions on Pattern Analysis and Machine Intelligence, pp.629-639, 1990.

[14] M. Gürelli and C. Nikias, *An eigenvector-based algorithm for multichannel blind deconvolution of input colored signals*, IEEE Transaction of Acoustics, Speech, and Signal Processing, pp.134-149, 1995.

[15] G. Harikumar and Y. BreŠler, *Perfect blind restoration of images blurred by multiple filters: theory and efficient algorithms*, Visual Communications and Image Processing, pp.1819-1830, 2005.

[16] Y. Chen,Y. Luo and D. Hu, *A general approach to blind image super-resolution using a PDE framework*, IEEE Transactions on Image Processing, 8(2), pp.202-219, 1999.

[17] F. Šroubek,G. Cristobal and J. Flusser, *Simultaneous super-resolution and blind deconvolution*, Journal of Physics: Conference Series, 124, 2008.

[18] U. Engelke and H. J. Zepernick, *Perceptual-based quality metrics for image and video services: a survey*, Next Generation Internet Networks, pp.190, 2007.

[19] R. Barland and A. Saadane, *Reference free quality metric for JEPG-2000 compressed images*, Information Technology Journal, 2006.

[20] P. Marziliano, F. Dufaux, S. Winkler and T. Ebrahimi, *Perceptual blur and ringing metrics: application to JPEG2000*, Signal Processing: Image Communication, pp.163-172,2004.